Water Management along the Flow Channels of PEM Fuel Cells

Jung S. Yi, J. Deliang Yang, and Constance King
UTC Fuel Cells, South Windsor, CT 06074

DOI 10.1002/aic.10307
Published online in Wiley InterScience (www.interscience.wiley.com).

Water management is one of the most critical issues for high-performance polymer-electrolyte-membrane (PEM) fuel cells. A water-flux model for vapor and liquid phases along a gas flow channel is developed. The dependency of the operating and design parameters, such as temperature, pressure, gas and liquid flow rate, and size of the fuel cell, on the water management along the flow channel is demonstrated. Issues associated with liquid water and membrane/electrode dry out as well as system water balance are identified. An "intracell" water-exchange method, which can remove or supply water within a cell depending on local demand, is described. This water management scheme effectively minimizes the issues described above. Good cell performance with a high limiting current at low reactant pressure and high reactant utilization is demonstrated with this advanced water management system. © 2004 American Institute of Chemical Engineers *AIChE J,* 50: 2594–2603, 2004

Keywords: PEM fuel cells, water management, mass transport, flow field, water transport plate

Introduction

The polymer-electrolyte-membrane (PEM) fuel cell has gained an enormous amount of attention as a power source (St-Pierre et al., 2001). Low cost and high power density are obtained with a low-temperature operation and with a membrane electrolyte that will not migrate as do liquid electrolytes. The sulfonated ion-exchange membrane transports protons across its thickness because of an electrical potential difference. Because proton mobility within the membrane strongly depends on the water content of the membrane the proton-exchange membrane must be well humidified within the fuel cell to maintain good proton conductivity (Gottesfeld, 1997). Generally, humidified reactant gases are used to maintain membrane humidity. Often, this requires an external component for the fuel cell system, and additional energy is expended to humidify the fuel stream. Alternative humidification schemes include internal membrane humidification by wicking or by platinum implantation in membranes, self-humidification with counter flow reactants, and liquid water injection. Reviews of the humidification techniques are provided by St-Pierre et al. (1997) and Wood et al. (1998).

The removal of water transported from the anode and generated at the cathode is also very critical. Once the gas stream becomes saturated, the water will exist in liquid form because the cell temperature is lower than the boiling point of water. The presence of liquid water can result in mass-transport limitations resulting from the restriction of oxygen transport through the gas-diffusion electrode and flooding of active catalyst sites, especially at high current density. Also, water within the gas-diffusion layer (GDL) and/or gas flow channels can result in a nonuniform distribution of reactants over the active catalyst area and among cells in a stack. This can result in both poor cell performance, and cell-to-cell performance variation within a stack. Therefore, managing water within the cell, not only to hydrate the membrane but also to minimize transport resistance, is a critical issue for high-performance PEM fuel cells.

Many researchers have investigated water distribution and behavior within each layer of the cell to minimize ohmic and mass transport resistances. Water retention and transport in the

Correspondence concerning this article should be addressed to J. S. Yi at jung.yi@utcfuelcells.com.

membrane were studied by Springer et al. (1991). Their model accounted for both electro-osmotic drag and diffusion of water through the membrane, from which they concluded that the net water transport through the membrane from anode to cathode could be insignificant relative to the amount of water generated. Bernardi and Verbrugge (1991, 1992) developed models, including reactant and water transport in the electrode, and estimated the hydraulic pressure profile through the electrode and membrane. A significant increase in hydraulic pressure at the electrode is predicted from their model. Recently, the temperature profile in the membrane and electrode was simulated by Rowe and Li (2001), predicting the effect of relative humidity on the energy distribution and, therefore, on the cell performance for various operating conditions.

Reactant transport through the GDL was also investigated by Bernardi and Verbrugge (1991, 1992) and by Springer et al. (1993). In their studies, only vapor-phase water transport was considered, using the Stefan–Maxwell diffusion equation, with an average reactant concentration in the gas flow channel. Many researchers have investigated the effect of the ribs of the gas flow field on the reactant diffusion in the GDL with various complexities (Kulikovsky et al., 1999; West and Fuller, 1996; Yi and Nguyen, 1995). Again, their studies were related to gas-phase diffusion only. Recently, Natarajan and Nguyen (2001) added the effect of capillary flow of liquid water within the GDL on the gas diffusion through the GDL, including the presence of channel and rib area. In those studies, various degrees of transport resistance through the GDL are reported as the result of the various assumptions used in each model. To reduce mass transport resistance, the gas-diffusion media may be configured to function in the presence of liquid water and to expel liquid water. As an example, convective gas flow through the GDL has been proposed not only to improve the reactant transport rate, but also to push liquid water out from the GDL to the gas flow channel by modifying the flow field to have interdigitated dead-ended channels (Amakawa and Uozumi, 1986; Ledjeff et al., 1993; Nguyen 1996; Wilkinson et al., 1993; Wilson, 1997). The effects of interdigitated convective flow was also theoretically studied by considering the gas phase only (Kazim et al., 1999; Yi and Nguyen; 1999), and by including the presence of liquid water (He et al., 2000). Much better utilization of the area under the rib due to faster reactant transport is reported from those studies. A similar convection effect was also reported by using the serpentine flow field design (Dutta et al., 2001; Kulikovsky, 2001). Changes of the GDL hydrophobicity also have been proposed to improve mass transport in the GDL (Mueller et al., 1998). Liquid water drawn from the cathode to the anode through the membrane by a water vapor partial pressure gradient has also been investigated (Wilkinson et al., 1994).

After water is transported from GDL to the flow channels, it still must be removed from the stack along the gas flow channel. Therefore, water management along the gas flow channel is also important for developing an effective water management PEM fuel cell design. To understand water transport behavior in the flow channels, numerous models of PEM fuel cells describing the water transport phenomenon along the gas flow direction have been developed. Fuller and Newman (1993) described the water vapor effect on gas concentration along the reactant flow direction for various flow rates and demonstrated that water and thermal management are tightly interrelated. Kimble and Vanderborgh (1992) modeled the effect of the presence of liquid water on the reactant concentration profile along the channel as a consequence of temperature profile changes. Nguyen and White (1993) studied the cell performance for various humidification and heat removal designs simulating gas- and liquid-phase flows along the channel. Wang et al. (2000) also modeled gas and liquid water profiles along the flow channels. However, thermal effects associated with vaporization and condensation were not included in Wang's model. To evaluate various operating conditions on cell performance, a multicomponent, two-phase fuel cell model was developed by Yi and Nguyen (1998). Their study evaluated different coolant flow schemes, and they concluded that the counter-coolant flow is preferable for thermal and water management purposes, as did St-Pierre et al. (1997). The models discussed above did not consider the pressure changes along the flow channel; however, the effect of pressure change along the channel has been studied by other research groups (Dutta et al., 2000, 2001; Futerko and Hsing, 2000; Gurau et al., 1998; Kulikovsky, 2001). Gurau et al. (1998) modeled hydrodynamics along the gas flow path using the Navier–Stokes equation, claiming that some of the convective flow along the gas flow channel penetrates into the GDL. Dutta et al. (2000, 2001) developed three-dimensional models and simulated a complete cell with a straight flow field as well as a serpentine flow field. However, effects of temperature distribution, which are very closely coupled with pressure changes and very critical for water management, were not included in the pressure models presented above.

In this communication, water vapor removal and liquid water flow within the cell are mathematically described and related to the temperature and pressure profiles along the gas flow channels. The critical issues related to water management in designing fuel cell stacks are discussed. Then, the intracell water-exchange system used at UTC Fuel Cells is demonstrated as a liquid water removal scheme as well as for membrane humidification. The effectiveness of this system is discussed, demonstrated, and related to water management in PEM fuel cells.

Water Vapor Flow along a Gas Flow Channel

When water is formed in the electrode, it must be transported out either through the GDL to the gas channel or through the membrane toward the other electrode. The effectiveness of water removal affects the reactant transport resistance in the electrode and GDL. The change of water content also affects the ohmic resistance of the membrane. Because understanding of the water management phenomena along the reactant streams is the aim of this paper, it is expedient to treat both the catalyst layer and the gas-diffusion layer as a single interface by assuming that water is transported effectively through the layers. Then the water vapor flow along the gas stream is mathematically modeled to describe the phase-exchange phenomenon of water along the channel resulting from condition changes. The simplified schematic of the modeled domain is shown in Figure 1. From a material balance for water vapor in a volume element of a gas flow channel, the molar flux of water exchanged from the gas stream perpendicular to the plane of the electrode (N_s) is derived, and is represented as

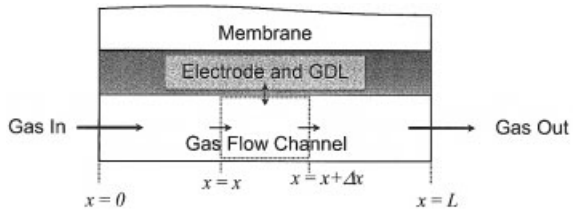

Figure 1. Modeled domain.

$$N_s = N_{gen} + N_{drag} - h\frac{dN^v}{dx} \tag{1}$$

where N_{gen} is water generation attributed to reaction. Therefore, it can be written as

$$N_{gen} = \frac{i}{2F} \qquad \text{for cathode} \tag{2a}$$

$$N_{gen} = 0 \qquad \text{for anode} \tag{2b}$$

and the water dragged through the membrane (N_{drag}) is

$$N_{drag} = \alpha\frac{i}{F} \qquad \text{for cathode} \tag{3a}$$

$$N_{drag} = -\alpha\frac{i}{F} \qquad \text{for anode} \tag{3b}$$

where i is the current density, F is the Faraday's constant, and α is the net water transport coefficient through the membrane from anode to cathode. Here, a constant current density along the flow channel is assumed, and the average value of the net transport coefficient of water is used. The third term in the right side of Eq. 1 describes the molar flux change of water vapor ascribed to temperature and pressure variations, where h is the depth of the gas flow channel and N^v is the molar flux of water vapor. The molar flux of water vapor can be expressed in terms of vapor pressure as the following

$$\frac{N^v}{N^v + \Sigma_j N_j} = \frac{p_w^v}{p} \tag{4}$$

where p is the total gas pressure in the channel, N_j is the dry gas flux of the specie j in the channel at a given location, and p_w^v is the vapor pressure of water at a given temperature (T). An empirically correlated equation expressing the dependency of water vapor pressure on temperature is used (Felder and Rousseau, 1986). The dry gas flux can be written as the following, assuming uniform current distribution along the channel

$$\sum_j N_j = \frac{i(c+r)}{nFch}\left(\frac{L}{Uy_{in}} - x\right) \tag{5}$$

where c is the channel width, r is the rib width of the gas flow channel, L is the total length of the channel, n is the number of electrons used for a mole of reactant, U is the reactant utilization, and y_{in} is the supplied dry reactant concentration. Therefore, the water balance equation for the anode and cathode can be written as

$$N_s = \frac{i}{2F} + \frac{\alpha i}{F} + \frac{i}{4F}\frac{c+r}{c}\left(\frac{\frac{p_w^v}{p}}{1-\frac{p_w^v}{p}}\right) - \frac{h\,\Sigma_j N_j}{p}\frac{\left(\frac{dT}{dx}\frac{dp_w^v}{dT} - \frac{p_w^v}{p}\frac{dp}{dx}\right)}{\left(1-\frac{p_w^v}{p}\right)^2} \qquad \text{for cathode} \tag{6a}$$

$$N_s = -\frac{\alpha i}{F} - \frac{i}{2F}\frac{c+r}{c}\left(\frac{\frac{p_w^v}{p}}{1-\frac{p_w^v}{p}}\right) - \frac{h\,\Sigma_j N_j}{p}\frac{\left(\frac{dT}{dx}\frac{dp_w^v}{dT} - \frac{p_w^v}{p}\frac{dp}{dx}\right)}{\left(1-\frac{p_w^v}{p}\right)^2} \qquad \text{for anode} \tag{6b}$$

Here, the third term in Eq. 6a is the condensation of water attributed to the pressure change caused by the consumption of oxygen by reaction, and the last term is the water vapor flux change resulting from temperature and pressure changes along the gas flow channel. The terms in Eq. 6b are analogous. Therefore, for given temperature and pressure profiles along the gas flow channel, the required flux of water exchanged from the vapor water stream can be calculated with contributions attributed to reaction, drag, pressure, and temperature changes. If N_s is positive, it means that liquid water is condensed from the gas stream, and a negative N_s means that water needs to be vaporized to maintain saturation of the gas stream.

In the cathode, water is supplied by generation and transportation through the membrane. Thus the first and the second terms of Eq. 6a are positive. Here, a positive net transport coefficient (α) is used for this calculation (Ren and Gottesfeld, 2001; Springer et al., 1991; Yi and Nguyen, 1998). As the reactant stream flows along the channel, the reactant flux will be decreased because of consumption, indicating that the third term of Eq. 6a will contribute to the condensation of water from the gas stream. Therefore, to manage the water condensation or vaporization rate locally for a given operating condition, the temperature gradient (dT/dx) and pressure gradient (dp/dx) in the last term are the only control parameters. It needs to be pointed out that the temperature gradient and the pressure gradient are affected by the energy used for phase change of water and by the amount of water present in the channel, respectively.

Figures 2 and 3 show the required temperature profile to supply or eliminate water from the cell using the vapor stream without any liquid water condensation in the channel or membrane/electrode dry out ($N_s = 0$). A linear pressure profile is used for this calculation. The pressure profile can be manipulated by the size and type of the gas channels. Also, for a given

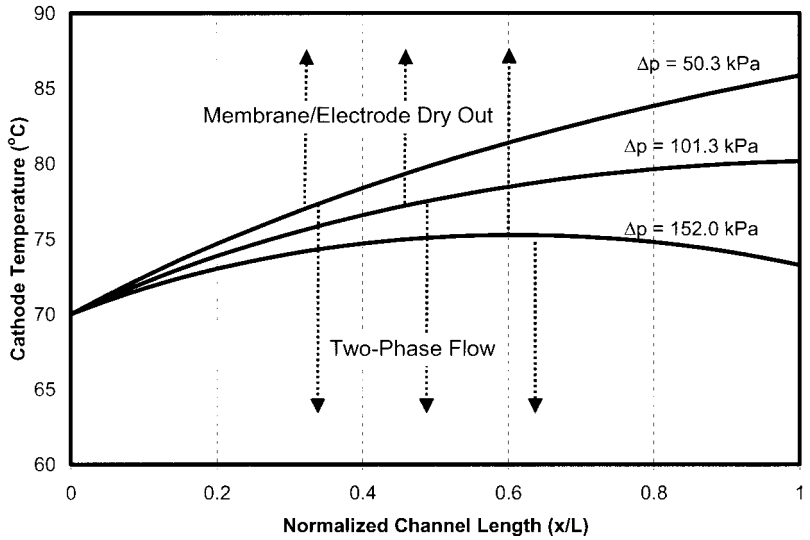

Figure 2. Air cathode temperature profiles required for single-phase operation of PEM fuel cells.

i = 1.0 A/cm^2, α = 0.1, h = 0.5 cm, p_{in} = 304 kPa, U_{O2} = 0.6.

flow channel design, the reactant gas utilization can be varied to change the pressure drop in the gas flow channel. Once the pressure gradient is determined, the required temperature gradient at any location can be calculated for a given inlet temperature, as shown in Figures 2 and 3. If a local temperature is higher than the temperature profile given in the figure at any point, it will lead to membrane/electrode dry out. If the temperature is lower than the profile calculated above, liquid water forms inside of the cell, causing a two-phase flow in the channel to occur. In other words, to prevent membrane/electrode dry out and the formation of liquid water, the temperature profile is fixed for a given flow field design and operating conditions. In the cathode, a continuously increasing temperature profile is required for relatively low pressure gradient cases as shown in Figure 2. However, the required temperature gradient starts to decrease as Δp increases. In the anode, a decrease in the temperature profile is required as shown in Figure 3. The temperature profile along the gas stream can be manipulated by arranging the reactant and coolant flow configurations (St-Pierre et al., 1997; Yi and Nguyen, 1998).

The reactant gas utilization can also be adjusted to change the temperature profile within the cell. In this simulation, a uniform current density and a constant net transport coefficient of the membrane are assumed along the gas stream. In operating fuel cells, the values may vary depending on the operating and design parameters. To prevent membrane/electrode dry out or two-phase flow, the required temperature profiles of the anode and the cathode may be different from the profile predicted in Figures 2 and 3. Precisely manipulating the temperature profile for each location in the flow field is not practical. In addition, trying to satisfy both the anode and cathode profiles at the same time is not realistic. Therefore, a two-phase

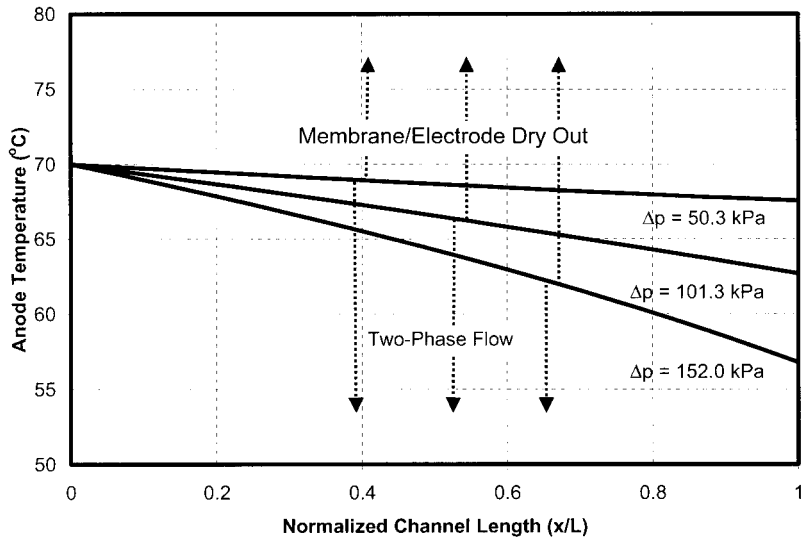

Figure 3. Anode required temperature profiles for single-phase operation of PEM fuel cells.

i = 1.0 A/cm^2, α = 0.1, h = 0.5 cm, p_{in} = 304 kPa, 50% H_2 reformate, U_{H2} = 0.8.

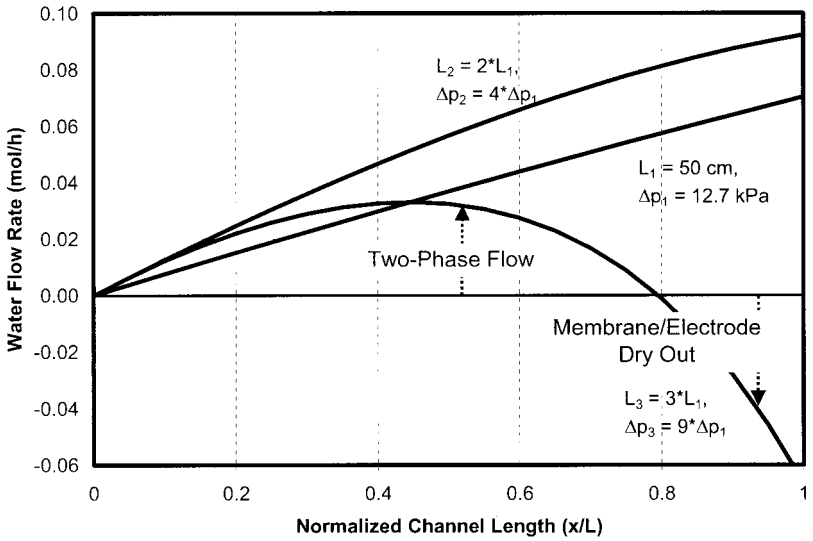

Figure 4. Effect of channel length on liquid water profile along the air cathode flow channel of PEM fuel cells.

i = 1.0 A/cm^2, α = 0.1, h = 0.5 cm, p_{in} = 304 kPa, T_{in} = 85°C, T_{out} = 65°C, linear temperature profile, U_{O2} = 0.6.

flow in the gas flow channels of a realistic fuel cell application is unavoidable.

Two-phase flow in reactant streams

The liquid water generated at a given location in the active area must be eliminated from the cell to prevent liquid water accumulation. With commonly used solid bipolar plates, the liquid water has to be carried along the flow channel. Therefore, the liquid water flow rate (M^l) is calculated by integrating the water condensation rate described by Eq. 6 over the channel distance (x) as shown below

$$M^l(x) = c \int_0^x N_s dx \tag{7}$$

where $M^l(x)$ is the liquid water flow rate at a given location to prevent any water accumulation. However, the liquid water flow rate is proportional to the gas flow rates and the water drag coefficient at the flow channel surface. If the liquid water flow is lower than the liquid water flow rate calculated in Eq. 7, then water droplets will stay on the surface of the flow channels, causing gas flow maldistribution. Therefore, the gas flow rates, the dimension, and the surface condition of the flow channels must be carefully selected to prevent water accumulation inside of the flow channel.

Figure 4 shows the flow channel scale up effects on the profile of the liquid water flow rate along the cathode flow channel. A fixed temperature difference between the inlet and outlet is applied, assuming the coolant flow of the stack can be managed to maintain the same temperature difference for various channel lengths. With an increasing channel length, the electrode area covered by the flow channel also increases; therefore, the ratio of the pressure drop increase in the flow channel is the squared amount of the increase in channel length for a fixed gas utilization (Perry et al., 1984). Three different channel lengths with corresponding flow field pressure drops are compared in Figure 4. The amount of liquid water flowing in the channel grows continuously along the channel with small cells. Higher water flow rate with the longer channel is observed for case L_2 compared to case L_1. However, a significant decrease in the liquid water flow rate is observed as the exit for the longer channel is approached (case L_3). This is because the effect of the pressure gradient becomes more significant as the channel length increases. Case L_3 shows that within a cell, it is possible to have both a region in excess of liquid water, indicated by a positive water flow, and a region with water deficit, indicated by a negative water flow. Flooding will take place in regions with excessive liquid water, and membrane/electrode dry out may occur in regions deficient of water.

In a fuel cell of practical size, temperature variations within a cell and among cells are unavoidable and result in different rates of liquid water formation. With the presence of liquid water droplets flowing along with the gas, the pressure drop in a gas flow stream increases. This causes reactant flow maldistribution from channel to channel. A gas maldistribution from cell to cell can also be created in a stack, resulting in lower cell performance. To resolve this issue, a high-pressure drop along the flow channel is required. To maintain a high-pressure drop between the inlet and the outlet of the channel, serpentine flow fields are commonly used (Stumper, 1998). The inlet reactant pressure must be sufficiently high enough to allow a high Δp. At the same time, a temperature profile has to be carefully selected so that local membrane/electrode dry out is minimized. Therefore, redesigning the flow field plates are required for scaling up a fuel cell stack.

Water Balance and System Design

Typically, hydrogen supplied to the fuel cell is completely consumed for a pure hydrogen system, and the residual amount of oxygen in the cathode stream is exhausted with inert gases. To maintain water balance, the amount of water exhausted from the system should be equal to the amount of water generated, expressed as

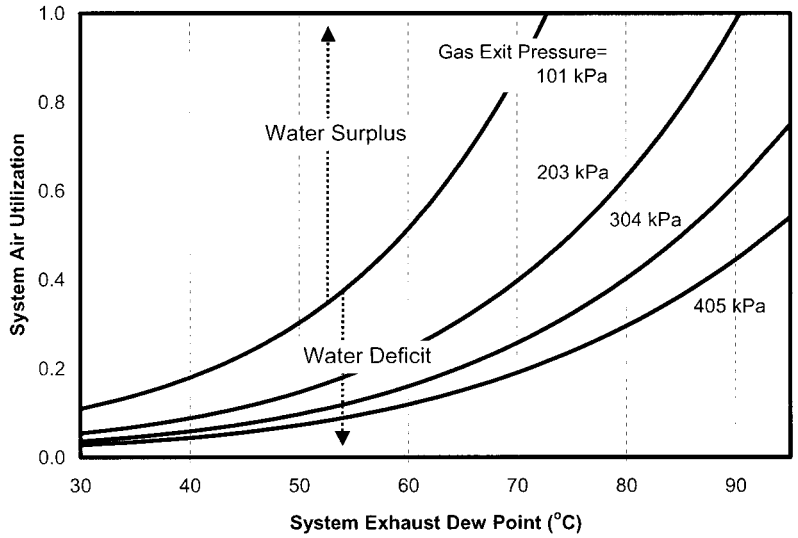

Figure 5. Effect of maximum air utilization on system exhaust dew point on various gas exit pressures for water balance of hydrogen/air fuel cell system.

$$M_{gen} = M^{v}_{exh} \tag{8}$$

where the water generation rate in the system can be described as

$$M_{gen} = N_{gen}A \tag{9}$$

where N_{gen} is the water generated as the result of the electrochemical reaction, which is defined in Eq. 2a, and A is the active area of the fuel cell stack. The water vapor exhaust rate (M^v) can be derived from Eq. 4 in relation to the exhaust dry gas flow rate (M^g_{exh}) and the water vapor pressure, which is a function of the exhaust dew temperature as shown below

$$M^{v}_{exh} = \frac{\dfrac{p^{v}_{w}}{p}}{\left(1 - \dfrac{p^{v}_{w}}{p}\right)} M^{g}_{exh} \tag{10}$$

The exhaust dry gas flow rate can be expressed as

$$M^{g}_{exh} = \frac{iA}{4F}\left(\frac{1}{U_{O2}y_{O2,in}} - 1\right) \tag{11}$$

By combining the above equations, a water balance equation is derived and is expressed as

$$U_{O2} = \frac{\dfrac{p^{v}_{w}(T)}{p}}{y_{O2,in}\left[2 - \dfrac{p^{v}_{w}(T)}{p}\right]} \tag{12}$$

As shown in Figure 5, net water will be lost from the system if the exhaust dew point is higher than the stated value in the figure with a fixed exhaust pressure and air utilization. Thus, a water recovery device is required to maintain water balance, resulting in increased volume and weight for the system. As Figure 5 shows, higher air utilization and higher exit pressure are preferred to allow a higher exhaust dew point. However, as the air utilization of the system increases, the cell performance decreases not only because of the decrease in average reactant concentration but mainly because of the increase in mass transport resistance related to water management, as discussed previously. The air pumping power also increases as the operating pressure increases and also as air utilization decreases, resulting in increasing the parasitic power of the system. Thus, it is often necessary to optimize a system based on its cell stack technology and its application, and the water management along the channel plays important roles in designing a fuel cell stack as well as an optimized fuel cell system.

Intracell Water-Exchange System

To eliminate water related issues in a PEM, an intracell water-exchange scheme is used at UTC Fuel Cells. Key to this water management system is the water transport plate (WTP), a porous bipolar plate in which the pores are filled with liquid water. The WTP is gas impermeable, similar to a regular bipolar plate, preventing gas ingestion to the coolant streams while allowing water exchange. This concept was proposed by Schutz (1989) in an Austrian patent. The idea of using a fine-pore WTP and its system concept was independently proposed, demonstrated, and adopted at UTC Fuel Cell (Meyer et al., 1996; Reiser, 1994, 1997). A schematic of the intracell water-exchange system is shown in Figure 6. The reactant gas streams are maintained at a higher pressure than the pressure in the coolant stream with a predetermined pressure difference between the gas and the coolant flow fields. This pressure difference causes excess liquid water in contact with the WTP to be wicked into the WTP and moved to the coolant passage network at a local level. The local water flux to the WTP is described by Eq. 6, the differential form, as opposed to Eq. 7, the integral form, that is used for the common solid bipolar

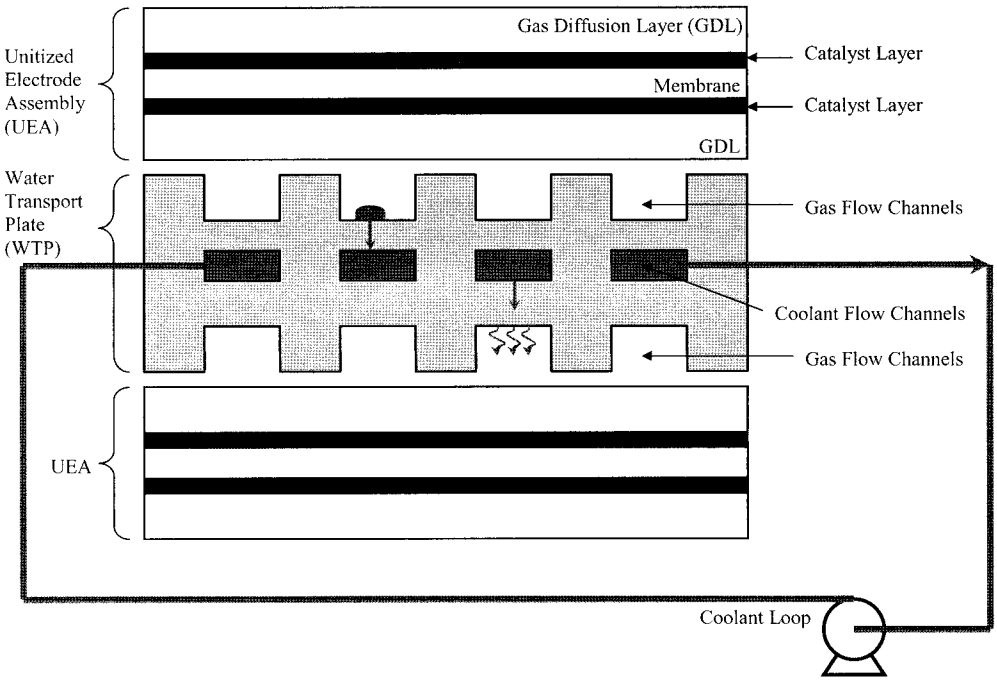

Figure 6. Within-cell water-exchange system used in UTC Fuel Cells.

plates. Thus, issues associated with liquid water accumulation along the channel are eliminated.

The effectiveness of liquid water removal is shown in Figure 7. The cell performance is plotted against the pressure difference applied between the reactant and the coolant stream. At low pressure differential, the cell performance is low, and the flow field pressure drop was observed to be higher than in the case with the higher pressure difference between gas flow channel and coolant flow channel. This indicates a two-phase flow occurring in the flow fields with the lower pressure differential. However, as the pressure differential increases, the cell performance increases. A maximum cell performance is observed after a certain pressure differential (Δp_{peak}). This pressure differential is the optimum driving force for differential liquid water removal.

Because liquid water is effectively removed from the reactant stream at a local level, the temperature and pressure constraints to prevent membrane/electrode dry out or two-phase flow in the gas flow stream are not applied for this system. Thus, the scale-up issues discussed previously for the regular bipolar plate also do not apply. Figure 8 shows the performance comparison for different sizes of fuel cell stacks with the intracell water-exchange method. No difference in performance is demonstrated among a single cell, a 20-cell

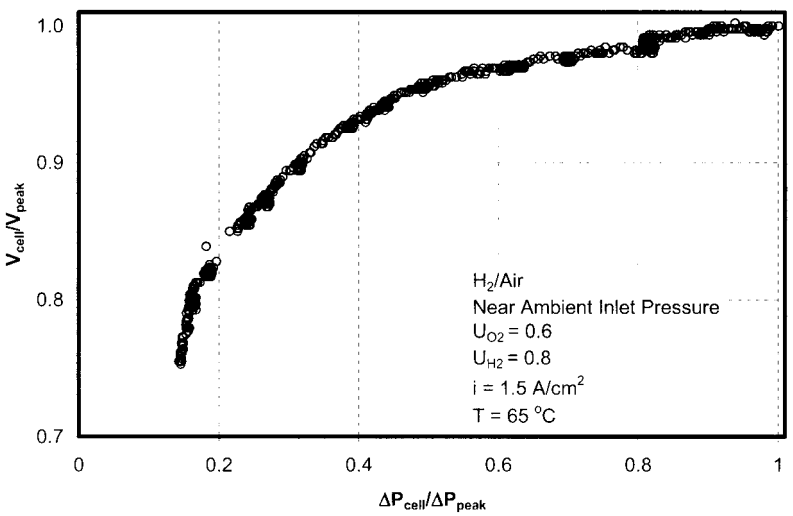

Figure 7. Effect of pressure difference applied between reactant stream and coolant stream on cell potential for the within-cell water-exchange stack.

H_2/Air, near ambient reactant pressure, 1.5 A/cm^2, U_{H2} = 0.8, U_{O2} = 0.6, 65°C.

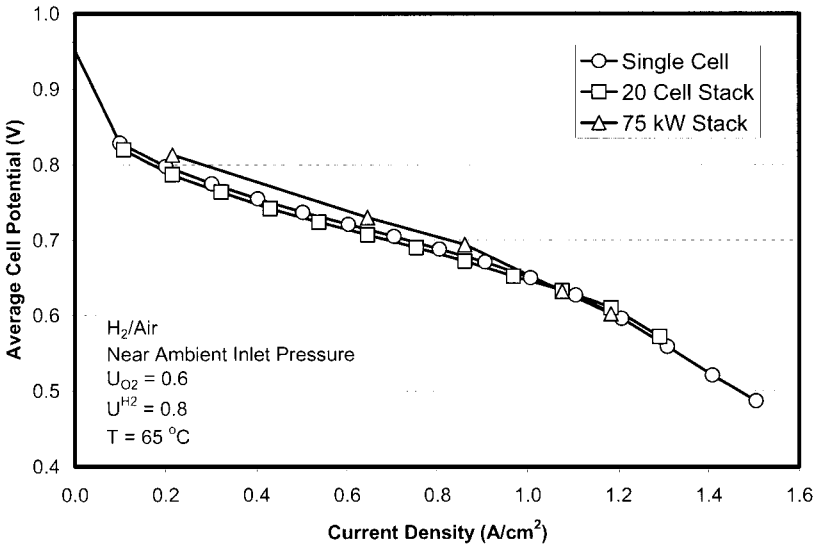

Figure 8. Comparison of stack size on cell performance for the UTC Fuel Cells within-cell water-exchange PEM fuel cell system.

H_2/Air, near ambient reactant pressure, 1.5 A/cm^2, $U_{H2} = 0.8$, $U_{O2} = 0.6$, 65°C.

stack, and a 75 kW stack, even though the temperature profiles are vastly different for those three cases.

In addition, because a high-pressure drop within the flow channel is not required for this water management method, near-ambient pressure operation is possible, allowing a simpler flow field design, and minimizing required parasitic power for air compression to maximize the overall system efficiency. By minimizing the mass transport resistance attributed to the presence of liquid water in the gas stream, operation at high air utilization is also possible without significant stack performance penalty. Figure 9 shows the oxygen utilization responses on cell potential at various high current densities. Figure 9 indicates that 70 to 80% oxygen utilizations are possible without significant performance loss at relatively high current densities with near-ambient inlet pressure operation. Even better utilization response is obtained at lower current densities.

Because liquid water is removed on a differential level, the stack can be used as a water recovery device. With 80% oxygen utilization, an ambient pressure hydrogen system can be in water balance if the cathode air exits the stack with a dew point equal to 68°C as shown in Figure 5. By arranging the cell stack so that the coolant enters the stack at about 68°C and leaves the cell stack at about 80 or 90°C, the system may be in heat and water balance without any external water recovery device.

In addition to the liquid water removal capability, when the reactant stream is dry, the water in the WTP pores spontane-

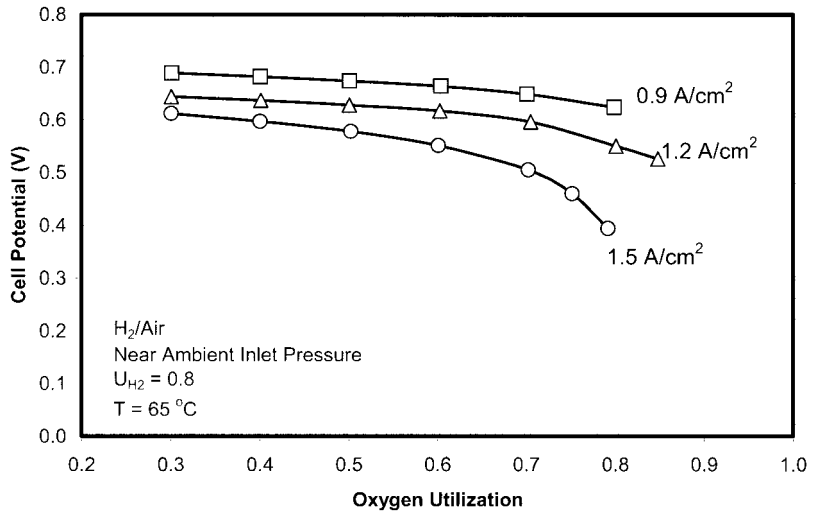

Figure 9. Effect of oxygen utilization on cell performance for full-size single cell with the within-cell water-exchange system.

H_2/Air, near ambient pressure, $U_{H2} = 0.8$, $T = 65$°C.

ously vaporizes to humidify the dry reactant stream. The pores maintain their water fill by capillary movement of water from the coolant channels (Bett et al., 1998). Therefore, water balance in every location of the cell is spontaneously achieved with intracell water removal or reactant humidification as needed.

Summary

Water flow along the channel was theoretically analyzed, and it was determined that a two-phase flow in the gas flow channel is unavoidable for a fuel cell stack of any practical size. The two-phase flow creates liquid water issues, especially when scaling up the stack for different applications. For good stack water management, lower reactant utilization, and higher pressure drop in the reactant stream are desirable. In contrast, higher reactant utilization and a lower pressure drop in the reactant are preferred for overall system efficiency and system water balance. Trade studies for these design and operating parameters are required to optimize the overall system.

At UTC Fuel Cells, an intracell water-exchange scheme is used with a fine-pore water transport plate. Humidification and water recovery are achieved within the cell, eliminating any external components. Furthermore, water removal is achieved within the cell on a differential level by applying a pressure difference between the reactants and coolant. Thus, high performance is achieved even with high reactant utilization, making ambient pressure operation possible.

Acknowledgments

The authors acknowledge Jonathan Puhalski and other UTC Fuel Cells associates for performing experiments. Also, we greatly benefited from the review and discussion of Drs. Shyam Kocha, John Bett, and Robert Darling.

Literature Cited

Amakawa, K., and N. Uozumi, "Fuel Cell," U.S. Patent No. 4 615 955 (1986).

Bernardi, D. M., and M. W. Verbrugge, "Mathematical Model of a Gas Diffusion Electrode Bonded to a Polymer Electrolyte," *AIChE J.*, **37**, 1151 (1991).

Bernardi, D. M., and M. W. Verbrugge, "A Mathematical Model of the Solid-Polymer-Electrolyte Fuel Cell," *J. Electrochem. Soc.*, **139**, 2477 (1992).

Bett, J. A., D. J. Wheeler, and C. Bushnell, "Porous Carbon Body with Increased Wettability by Water," U.S. Patent No. 5 840 414 (1998).

Dutta, S., S. Shimpalee, and J. W. Van Zee, "Three-Dimensional Numerical Simulation of Straight Channel PEM Fuel Cells," *J. Appl. Electrochem*, **30**, 135 (2000).

Dutta, S., S. Shimpalee, and J. W. Van Zee, "Numerical Perdition of Mass-Exchange between Cathode and Anode Channels in a PEM Fuel Cell," *Int. J. Heat Mass Transfer*, **44**, 2029 (2001).

Felder, R. M., and R. W. Rousseau, *Elementary Principles of Chemical Processes*, Wiley, New York (1986).

Fuller, T. F., and J. Newman, "Water and Thermal Management in Solid-Polymer-Electrolyte Fuel Cells," *J. Electrochem. Soc.*, **140**, 1218 (1993).

Futerko, P., and I.-M. Hsing, "Two-Dimensional Finite-Element Method Study of the Resistance of Membranes in Polymer Electrolyte Fuel Cells," *Electrochim. Acta*, **45**, 1741 (2000).

Gottesfeld, S., "Polymer Electrolyte Fuel Cells," *Advances in Electrochemical Science and Engineering*, Vol. 5, R. Alkire, H. Gerischer, D. M. Kolb, and C. Tobias, eds., p. 195 (1997).

Gurau, V., H. Liu, and S. Kakac, "Two-Dimensional Model for Proton Exchange Membrane Fuel Cells," *AIChE J.*, **44**, 2410 (1998).

He, W., J. S. Yi, and T. V. Nguyen, "Two-Phase Flow Model of the Cathode of PEM Fuel Cells Using Interdigitated Flow Fields," *AIChE J.*, **46**, 2053 (2000).

Kazim, A., H. T. Liu, and P. Forges, "Modeling of Performance of PEM Fuel Cells with Conventional and Interdigitated Flow Field," *J. Appl. Electrochem.*, **29**, 1409 (1999).

Kimble, M. C., and N. E. Vanderborgh, "Reactant Gas Flow Field in Advanced PEM Fuel Cell Design," Proc. of the 25th Intersociety Energy Conversion Engineering Conference, **V3**, 413 (1992).

Kulikovsky, A. A. "Numerical Simulation of a New Operation Regimes for a Polymer Electrolyte Fuel Cell," *Electrochem. Commun.*, **3**, 460 (2001).

Kulikovsky, A. A., J. Divisek, and A. A. Kornyshev, "Modeling the Cathode Compartment of Polymer Electrolyte Fuel Cells: Dead And Active Reaction Zones," *J. Electrochem. Soc.*, **146**, 3981 (1999).

Ledjeff, K., A. Heinzel, F. Mahlendort, and V. Peinecke, "Die Reversible Membrane—Brennstoffzelle," *VCH Verlagsgesellschaft*, 103 (1993).

Meyer, A. P., G. W. Scheffler, and P. R. Margiott, "Water Management System for Solid Polymer Electrolyte Fuel Cell Power Plants," U.S. Patent No. 5 503 944 (1996).

Mueller, B., T. Zawodzinski, J. Bauman, F. Uribe, and S. Gottesfeld, "Carbon Cloth Gas Diffusion Backings for High Performance PEFC Cathodes," *Proton Conducting Membrane Fuel Cells II*, S. Gottesfeld and T. F. Fuller, eds., p. 1 (1998).

Natarajan, D., and T. V. Nguyen, "A Two-Dimensional, Two-Phase, Multicomponent Transient Model for the Cathode of a Proton Exchange Membrane Fuel Cell Using Conventional Gas Distributor," *J. Electrochem. Soc.*, **148**, A1324 (2001).

Nguyen, T. V., "A Gas Distributor Design for Proton-Exchange-Membrane Fuel Cells," *J. Electrochem. Soc.*, **143**, L103 (1996).

Nguyen, T. V., and R. E. White, "A Water and Heat Management Model for Proton-Exchange-Membrane Fuel Cells," *J. Electrochem. Soc.*, **140**, 2178 (1993).

Perry, R. H., D. W. Green, and J. O. Maloney, *Perry's Chemical Engineers' Handbook*, Section 5, 6th Edition (1974).

Reiser, C., "Proton Exchange Membrane Fuel Cell Device with Water Transfer Separator Plates," World Patent Application WO94/15377 (1994).

Reiser, C. "Ion Exchange Membrane Fuel Cell Power Plant with Water Management Pressure Differentials," U.S. Patent No. 5 700 595 (1997).

Ren, X., and S. Gottesfeld, "Electro-osmotic Drag of Water in Poly(perfluorosulfonic acid) Membranes," *J. Electrochem. Soc.*, **148**, A87 (2001).

Rowe, A., and X. Li, "Mathematical Modeling of Proton Exchange Membrane Fuel Cells," *J Power Sources*, **102**, 82 (2001).

Schutz, P., "Fuel Cell," Austrian Patent 389 020 (1989).

Springer, T. E., M. S. Wilson, and S. Gottesfeld, "Modeling and Experimental Diagnostics in Polymer Electrolyte Fuel Cells," *J. Electrochem. Soc.*, **140**, 3513 (1993).

Springer, T. E., T. A. Zawodzinski, and S. Gottesfeld, "Polymer Electrolyte Fuel Cell Model," *J. Electrochem. Soc.*, **138**, 2334 (1991).

St-Pierre, J., and D. P. Wilkinson, "Fuel Cells: A New, Efficient and Cleaner Power Source," *AIChE J.*, **47**, 1487 (2001).

St-Pierre, J., D. P. Wilkinson, H. Voss, and R. Pow, "Advanced Water Management Techniques for Solid Polymer Fuel Cells," Proc. of the 2nd Int. Symp. on New Materials Fuel Cell Mod. Battery Syst. II, p. 318 (1997).

Stumper, J., S. A. Campbell, D. P. Wilkinson, M. C. Johnson, and M. Davis, "In-Situ Methods for the determination of Current Distribution in PEM Fuel Cells," *Electrochim. Acta*, **42**, 3773 (1998).

Wang, Z. H., C. Y. Wang, and K. S. Chen, "Two-Phase Flow and Transport in the Air Cathode of Proton Exchange Membrane Fuel Cells," *J. Power Sources*, **4094**, 1 (2000).

West, A., and T. F. Fuller, "Inference of Rib Spacing in Proton-Exchange Membrane Electrode Assemblies," *J. Appl. Electrochem.*, **26**, 557 (1996).

Wilkinson, D. P., H. H. Voss, and K. B. Prater, "Lightweight Fuel Cell Membrane Electrode Assembly with Interdigital Reactant Flow Passages," U.S. Patent No. 5 252 410 (1993).

Wilkinson, D. P., H. H. Voss, and K. B. Prater, "Water Management and Stack Design for Solid Polymer Fuel Cells," *J. Power Sources*, **49**, 117 (1994).

Wilson, M. S., "Fuel Cell with Interdigitated Porous Flow-Field," U.S. Patent No. 5 641 586 (1997).
Wood, D. L., J. S. Yi, and T. V. Nguyen, "Effect of Direct Liquid Water Injection and Integrated Flow Field on the Performance of Proton Exchange Membrane Fuel Cells," *Electrochim. Acta*, **43**, 3795 (1998).
Yi, J. S., and T. V. Nguyen, "The Effect of the Flow Distributor on the Performance of PEM Fuel Cells," *Proton Conducting Membrane Fuel Cells I*, S. Gottesfeld, G. Halpert, and A. Landgrebe, eds., p. 66 (1995).
Yi, J. S., and T. V. Nguyen, "An Along-the-Channel Model for Proton Exchange Membrane Fuel Cells," *J. Electrochem. Soc.*, **145**, 4 (1998).
Yi, J. S., and T. V. Nguyen, "Multicomponent Transport in Porous Electrodes of Proton Exchange Membrane Fuel Cells Using the Interdigitated Gas Distributor," *J. Electrochem. Soc.*, **146**, 38 (1999).

Manuscript received May 21, 2002, revision received Feb. 4, 2004, and final revision received Jun. 1, 2004.